Available online at https://li02.tci-thaijo.org/index.php/ssstj

Suan Sunandha Science and Technology Journal

Synthesis and Characterization of TiN Thin Films by DC Reactive Magnetron Sputtering

Siriwat Alaksanasuwan[1,3], Nirun Witit-anun[2,3]*

[1]Faculty of Science and Technology, Phranakhon Si Ayutthaya Rajabhat University, Phranakhon Si Ayutthaya 13000, Thailand
[2]Department of Physics, Faculty of Science, Burapha University, Chonburi 20131, Thailand
[3]Thailand Center of Excellence in Physics (ThEP), MHESI, Bangkok 10400, Thailand
***Corresponding author e-mail: nirun@buu.ac.th**

Received: *7 December 2022* / **Revised:** *11 May 2023* / **Accepted:** *19 June 2023*

Abstract

In this work, the titanium nitride (TiN) thin films were prepared on Si-wafers by using the DC reactive magnetron sputtering from a pure titanium target. The influence of N_2 flow rates, in the range of 1.0-4.0 sccm, on the as-deposited TiN film's structure was characterized by several techniques. (i) The crystal structures were studied by GI-XRD. (ii) The film's thicknesses, microstructures, and surface morphologies were analyzed by FE-SEM. (iii) The elemental composition of films was measured by EDS. (iv) The hardness was measured by the nano-indentation. (v) The color was identified by a UV-VIS spectrophotometer. The results showed that the as-deposited films were polycrystalline of B1-NaCl structure. The lattice constants were ranging from 4.211-4.239 Å. The as-deposited films showed a nano crystal size in the range of 17.8-24.6 nm. The thickness decreases from 1254 nm to 790 nm with following in the N_2 flow rates. The concentration of Ti and N depended on the N_2 flow rates. The cross-sectional analysis showed that the films had a compact-columnar structure. The hardness increased from 4 to 19 GPa with increasing in the N_2 flow rates. The close to the color of 24K gold thin films in the CIE L*a*b* system was obtained by deposition in optimal N_2 flow rates.

Keywords: TiN thin film, N_2 flow rates, Reactive magnetron sputtering

1. Introduction

The scientific research on the novel and high-performance industrialized materials are unstoppable. Many researchers from all over the world have pushed the performances of materials beyond their theoretical limits, in order to achieve the best results possible. Surface coating is one of the best ways to improve the materials' properties or durability, especially for those exposed to extreme working conditions and aggressive environments (Santecchia et al., 2015).

Hard coatings or hard thin films based on metals, ceramics, and related compounds have been utilized often during the past few decades as a surface treatment for effectively enhancing structural performance (Gao & Sun, 2019). Many of the hard coatings based on transition metal nitrides (such as TiN, CrN, and ZrN) have been investigated and widely used in surface modification, which is now common material in the coating industry (Mitterer, 2014).

Among these coatings, titanium nitride (TiN) is very interesting due to its very hard and chemically resistant ceramic material that has long been used for corrosion, erosion, and wears protective coatings (Jithin, Ganapathi, Vikram, Udayashankar, & Mohan, 2018). TiN is widely used in many applications, such as coated on cutting tools. Additionally, TiN exhibits biocompatible qualities leading to its usage in medical implants such as orthopedic and dental prosthesis.

TiN film is a well-known hard coating that has crystallized in the B1-NaCl structure, which is a solid solution as the nitrogen concentration is in the range of 37.5-50.0% (Santecchia et al., 2015). Nowadays, TiN is mainly used as a coating material in order to extend the lifespan of cutting tools that are made of high-speed steels or sintered carbides. As compared to the non-modified cutting tools, the use of TiN films allows an increase in the cutting speed and feed during machining (Lepicka et al., 2019). Typically, the TiN showed beautiful colored films: pale yellow, gray, brownish yellow, or red which depending on the stoichiometry. The TiN film

Suan Sunandha Science and Technology Journal

has a high hardness ranging from 20-22 GPa, and excellent thermal and mechanical stability (Grosso et al., 2017).

There are many methods of physical vapor deposition (PVD) and chemical vapor deposition (CVD) that have been used to deposit TiN films. Nevertheless, CVD requires the use of high substrate temperature (in excess of 900°C); which is not appropriate for sensitive substrates (Kumar, Kumar, Kalaiselvam, Thangappan, & Jayavel, 2018). In contrast, the PVD method uses a lower substrate temperature (around 400-550°C). Generally, PVD involves the deposition of Ti atoms on the substrate surface by sputtering or evaporation followed by a subsequent reaction with nitrogen at the substrate surface (Kim et al., 2009). Among this PVD, reactive magnetron sputtering is a commonly used technique to deposit thin films for surface uniformity and good adhesion (Thampi, Bendavid, & Subramanian, 2016).

It is well known that the quality of the sputtered deposited thin films depends upon several parameters such as nitrogen concentration in the chamber during deposition, sputtering power, base pressure, working pressure, substrate temperature, gas flow rates, and bias voltage (Ponon et al., 2015). These parameters included the N_2 flow rate used for deposit films are known to impact the grain growth and crystallographic orientation, which result in microstructure and properties of the as-deposited films (Ajenifuja, Popoola, & Popoola, 2019). It has been reported that the microstructure, surface morphology, and preferred orientation of TiN thin films deposited by reactive magnetron sputtering are mainly controlled by the ratio of deposited nitrogen ions to titanium atoms, which is vital to determine the performance of the films (Zhang et al., 2019). For example, the N_2 flow rate is strongly impacted on the grain size, crystal orientation and chemical state of TiN films. The results showed that the grain size and atomic ratio of N/Ti decreased with increase of the N_2 flow rate and the diffraction peak were reformed as (111) to (200) orientation (Zhou, Liu, Zhang, Ouyang, & Suo, 2016). Moreover, many properties of the hard nitride films such as hardness, stoichiometry or wear resistance may depend on the concentration of nitrogen in the film (Zhang et al., 2019).

The aim of this work is to study the effects of N_2 flow rates on the structure of TiN films, which are prepared by the reactive DC magnetron sputtering. The main characteristics of the as-deposited films such as crystal structures, microstructures, surface morphologies, and elemental compositions as well as the hardness and the color were investigated. The results of this research would be useful for the hard coating industrial applications.

2. Materials and Methods

2.1 Thin films preparation

The TiN thin films were deposited on Si wafers substrates by the homemade DC reactive unbalanced magnetron sputtering system, which is shown in Figure 1. A pure titanium disc of 50 mm in diameter and 3 mm in thickness served as the sputtering target and was mounted on a magnetron cathode that cooled by water. Prior to deposited thin films, all substrates were cleaned with acetone in an ultrasonic container for 10 min. Subsequently, they were rinsed in deionized water and dried with N_2 gas. After cleaning, the substrates were immediately inserted into the sample holder in the deposition chamber. The target-to-substrate distance was at 100 nm. The high purity of Ar (99.999%) and N_2 (99.999%) were used as the sputtering gas and reactive gasses, respectively. The Ar flow rate was set as a constant value of 20 sccm. Whereas in this work, the N_2 flow rates were set as a variable parameter in the range of 1.0-4.0 sccm, which was controlled by mass flow controllers.

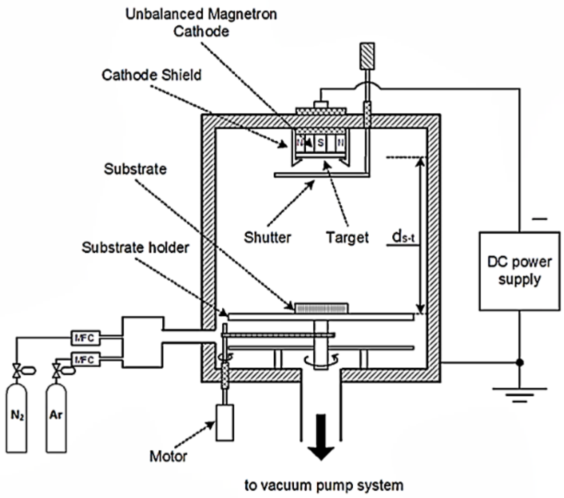

Figure 1. The homemade DC magnetron sputtering coater diagram.

Suan Sunandha Science and Technology Journal

Table 1. Thin films deposition conditions.

Parameters	Details
Sputtering target	Ti (99.97%)
Substrate temperature	room temperature
Target to substrate distance	100 mm
Base pressure	5.0×10^{-5} mbar
Working pressure	5.0×10^{-3} mbar
Sputtering power	300 W
Ar flow rate	20 sccm
N_2 flow rates	1, 2, 3, 4 sccm
Deposition time	30 min

Prior deposition the chamber was evacuated to a base pressure of 5.0×10^{-5} mbar by a diffusion pump backed with a rotary pump, before feeding the working gasses (Ar and N_2). The coating system employed an unbalanced magnetron powered by a homemade DC power supply. Before starting the deposition, the target was pre-sputtering for 5 min, with a shutter between the target and the substrate. During all depositions, the total working pressure and the sputtering power were kept fixed at 5.0×10^{-3} mbar and 300 W, respectively. The deposition time for each film was 30 min. The deposition conditions shown in Table 1.

2.2 Thin films characterization

The phase and crystal structures of the as-deposited films were analyzed by grazing incidence X-ray diffraction (GIXRD: BRUKER D8) in the continuous scanning mode using Cu Kα radiation (λ=0.154 nm). The diffraction angles were in the range of 20 - 80°. Scanning speed and grazing incidence angle was 2°/min and 3°, respectively. The crystal size can be calculated from the FWHM data acquired from the XRD pattern using Scherrer's equation. The microstructure, surface morphologies, cross-sectional morphologies, and thickness of the films were observed by a field emission scanning electron microscope (FE-SEM: Hitachi s4700). The composition of the films is examined by energy-dispersive X-ray spectroscopy (EDS: EDAX). The film's colors are measured by the UV-VIS spectrophotometer (UV-VIS: Shimadzu UV2600) in CIE L*a*b* system. The hardness was measured from a nanoindentation system (BRUKER: Hysitron TI Premier) at room temperature. The indentation was performed by using a Berkovich indent probe under depth-control mode. The indentation depth was controlled less than 1/10 of the film thickness, so that the influence from the substrate can be neglected, with maximum load at 9 mN.

3. Results and Discussion

3.1 Crystal structure

In this work, the as-deposited TiN thin films were successfully prepared on the substrates at room temperature by the reactive DC unbalanced magnetron sputtering, with N_2 flow rates ranging from 1.0-4.0 sccm. The crystal structure of as-deposited thin films was identified by the XRD technique at different N_2 flow rates presented in Figure 2. The results are showing that several diffraction peaks appeared at 2θ of 36.7°, 42.6°, 61.9°, and 74.1°. It corresponded to the polycrystalline of TiN at (111), (200), (220), and (311) planes (JCPDF no. 65-2899). The diffraction angles which corresponded to standard planes were found at N_2 flow rates of 1.0-4.0 sccm as the aberration of angles about ±0.3° for the as-deposited films. It has been shown that the crystal structure of films was a good agreement from the JCPDS standard.

Moreover, it was found the changing intensities of a diffraction peak with varying of the N_2 flow rates. As the lowest N_2 flow rates (1.0 sccm), the as-deposited thin films showed the low-crystallinity. The several phases appeared as the N_2 flow rates increased to 2.0 sccm, which corresponded to the polycrystalline of TiN at (111), (200), (220), and (311) planes. These phases still appeared as the N_2 flow rate increased to a higher value, but it showed an obviously preferred orientation of (111). The results showed that the orientation growth behavior was strongly related to the N_2 flow rate in the sputtering process. Additionally, the preferred orientations were controlled by the opposition of surface energy and strain energy. For example, the lowest surface energy caused to the (200) preferred orientation, whereas the lowest strain energy caused to the (111) preferred orientation (Pelleg, Zevin, Lungo, & Croitoru, 1991). In this work, the crystal sizes were analyzed by using the Scherrer formula from the FWHM of the XRD peaks; it was found that the crystal sizes of films ranged from 17.8 to 24.6 nm. The lattice constants of the films were in the range of 4.211-4.239 Å *(*the lattice constants of standard TiN are 4.238 Å*)*, which confirmed that the obtained films were complete of TiN structure.

Suan Sunandha Science and Technology Journal

In this work, the variation of N_2 flow rates is the result of the growing of crystallinity for the TiN films. In summary, the crystal sizes and the lattice constants of the films are shown in Table 2.

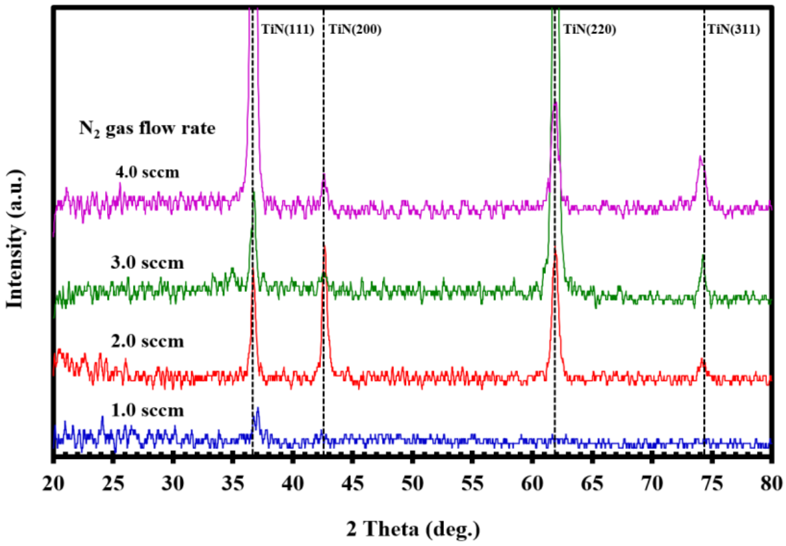

Figure 2. XRD pattern of the TiN thin films deposited at different N_2 flow rates.

Table 2. Crystal size and lattice constant of the as-deposited TiN thin films at different N_2 flow rates.

N_2 flow rates (sccm)	Crystal size [nm]				Lattice constants [Å]			
	(111)	(200)	(220)	(311)	(111)	(200)	(220)	(311)
1.0	17.8	-	-	-	4.211	-	-	-
2.0	22.6	21.3	19.7	19.2	4.234	4.234	4.236	4.234
3.0	23.9	20.3	21.5	23.2	4.233	4.239	4.235	4.234
4.0	24.6	20.3	20.1	20.3	4.233	4.233	4.236	4.237

3.2 Microstructure and surface morphology

Figure 3 showed the microstructure and surface morphology of the as-deposited TiN films at different N_2 flow rates ranging from 1.0-4.0 sccm. It is clearly presented that the films had a small grain and smooth surface, when deposited at the lowest N_2 flow rates as shown in Figure 3(a). Whereas the different sizes of the large grains were randomly distributed on the film's surface, when deposited at higher N_2 flow rates (Figure 3(b) to 3(d)). As the N_2 flow rate increased, the grain's size on the surface of the as-deposited film became smaller compared to the film deposited at a low N_2 flow rate. The result in this work may be described by the fact that the increase in N_2 flow rate declines the energy of bombarding ions, reduces the mobility of sputter atoms, and decreases the grain size (Zhou et al., 2016).

The cross-sectional analysis of the as-deposited TiN thin films observed by FE-SEM presented in Figure 4. It was revealed that the film's thickness decreased from 1254 to 790 nm with an increase in the N_2 flow rates (Table 3). It has been revealed that increasing the N_2 flow rates reduced the deposition rate. This effect is well known as for the reactive sputtering, the increasing of reactive gas during the deposition process intensely reduces the sputtering yield of a Ti-target due to target poisoning. On the other hand, since the concentration of the gas mixture was constant, an increase in the concentration of nitrogen followed by a decrease in the concentration of argon. Therefore, the sputtering yield of the target was reduced owing to the lower momentum transfer of nitrogen compared to argon (Zhang et al., 2000).

The as-deposited TiN thin films showed the dense structure at the N_2 flow rate of 1 sccm (Figure 3). When the N_2 gas flow rate increased to 2.0 sccm, the columnar structure appeared. It still achieved deposits at 3.0 and 4.0 sccm. This structure continuously grows throughout the thin film's growth, which corresponds to the zone 2 of the Thornton's structure zone model (SMZ) (Kusano, 2019). The columns are less defective and regularly facet at the surface of films. In summary, the microstructure of the TiN films in this work also show dense to compact-columnar.

Suan Sunandha Science and Technology Journal

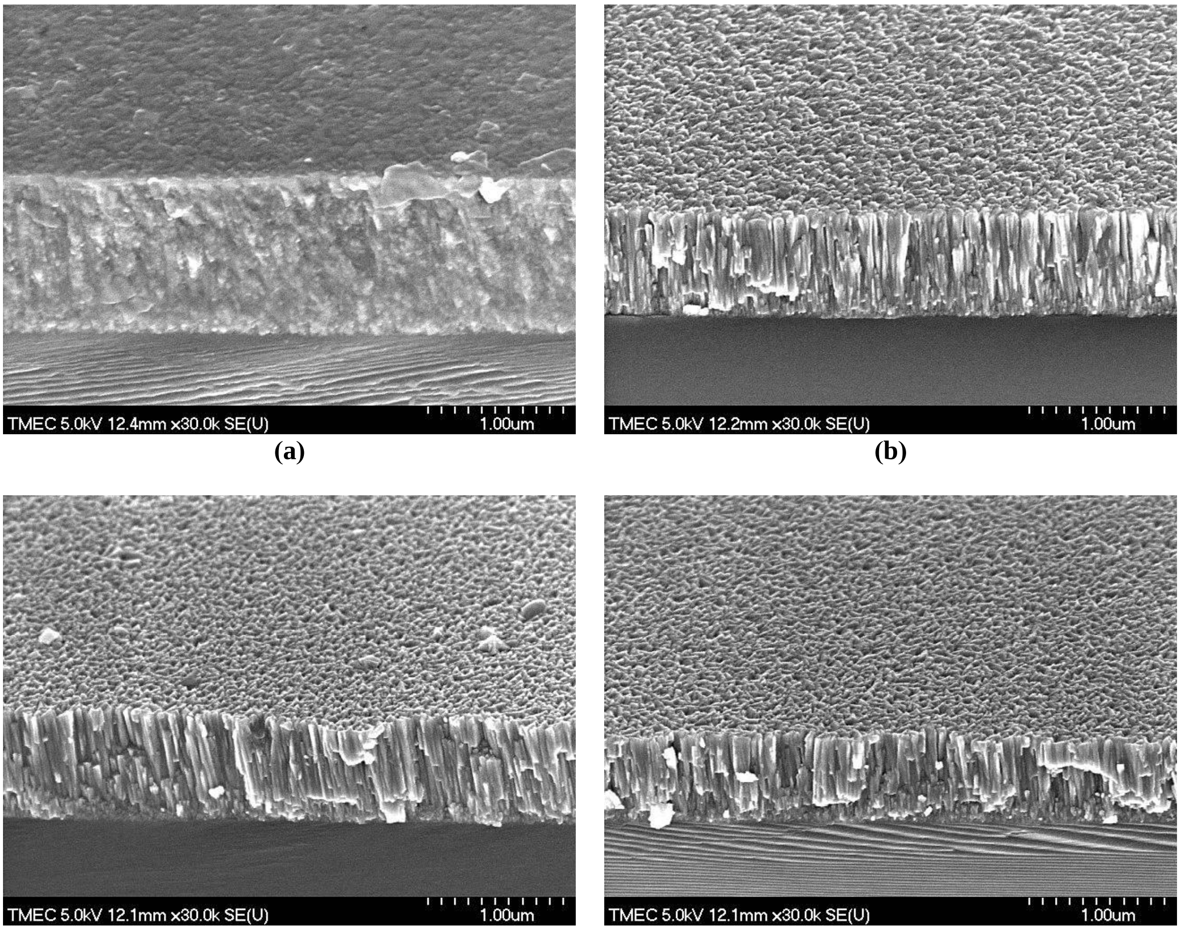

(a) **(b)** **(c)** **(d)**

Figure 3. FE-SEM micrograph of TiN thin films deposited at different N_2 flow rates; (a) 1.0 sccm, (b) 2.0 sccm, (c) 3.0 sccm, (d) 4.0 sccm.

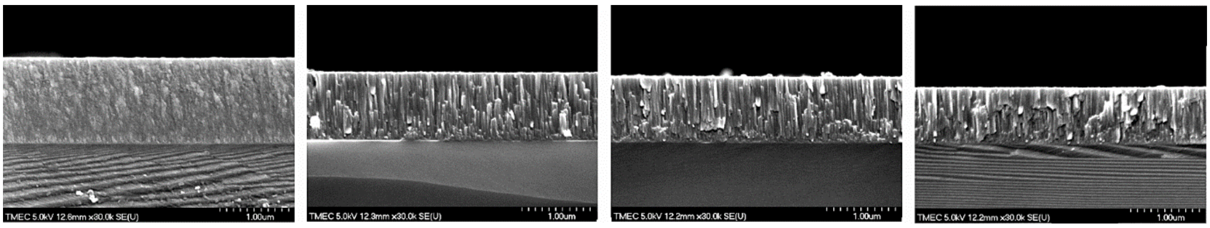

(a) **(b)** **(c)** **(d)**

Figure 4. Cross-sectional analysis of TiN thin films deposited at different N_2 flow rates; (a) 1.0 sccm, (b) 2.0 sccm, (c) 3.0 sccm, (d) 4.0 sccm.

Table 3. Some properties of the TiN thin films with different N_2 flow rates.

N_2 flow rate (sccm)	Thickness (nm)	Deposition rate (nm/min)	Structure	Hardness (GPa)	Color
1.0	1254	42	dense	4.5	grey
2.0	991	33	columnar	18.7	like-gold
3.0	865	29	columnar	19.0	like-gold
4.0	790	26	columnar	19.4	like-gold

Suan Sunandha Science and Technology Journal

3.3 Elemental composition

The elemental composition of the TiN thin films at various N_2 gas flow rates was analyzed by the energy dispersive spectroscopy (EDS) shown in Table 4 the N content increased from 43.8 to 53.7 at.% following on N_2 flow rates from 1.0 to 4.0 sccm. Actually, in this work, the Ti content decreased from 56.2 to 46.3 at.%, oppositely to the N content. Moreover, it also shows the ratio x of Ti content defined as x is Ti/(Ti+N), the ratio y of N content defined as y is N/(Ti+N), and the film composition defined as Ti_xN_y, respectively. It was found that the ratio of Ti and N content of films deposited at N_2 gas flow rate of 2.0 to 4.0 sccm was equally values of about 0.5 leading to the film composition in these cases being $Ti_{0.5}N_{0.5}$. Additionally, the ratio of Ti:N was approximately 1 indicating that the as-deposited TiN thin films in this case were stoichiometry.

Table 4. Elemental composition and film composition as a function of the N_2 gas flow rates.

N_2 flow rate (sccm)	Ti (at. %)	N (at. %)	x (Ti/Ti + N_2)	y (N/Ti + N_2)	Films composition (Ti_xN_y)
1.0	56.2	43.8	0.6	0.4	$Ti_{0.6}N_{0.4}$
2.0	47.2	52.8	0.5	0.5	$Ti_{0.5}N_{0.5}$
3.0	46.9	53.1	0.5	0.5	$Ti_{0.5}N_{0.5}$
4.0	46.3	53.7	0.5	0.5	$Ti_{0.5}N_{0.5}$

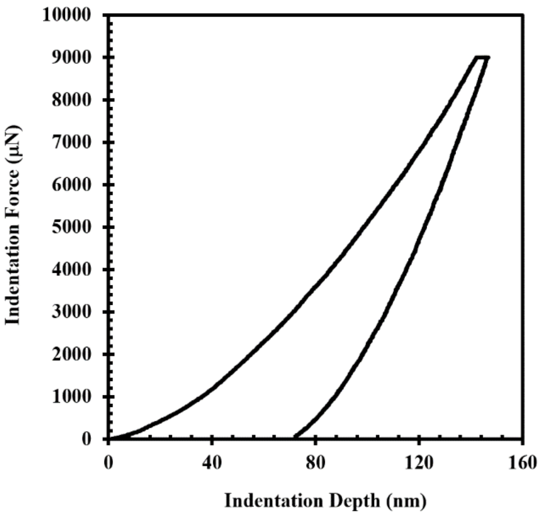

Figure 5. Sample of the load-displacement curve of TiN thin films.

3.4 Hardness

The hardness of TiN films was calculated from the load-unload displacement curve (Figure 5) and Table 3. It is accepted that the ratio of the indentation depth is around tenth of the total thickness by the nano-indentation technique.

In this study, the hardness was calculated for each unloading curve with values of 4.5 to 19.4 GPa. The maximum hardness of TiN films achieved to deposit at the highest N_2 flow rates (4.0 sccm), which showed the highest crystallinity of TiN (111). These results are consistent with another study. Zhang et al. (2019) reported that the TiN thin film with a high N_2 gas flow rate showed an obvious preferred orientation of TiN (111), which is the close-packed plane in the face-centered-cubic (fcc) crystal structure. Thus, at the high N_2 gas flow rate, TiN film showed the lowest compressive residual stress among other films.

3.5 Color

The as-deposited thin film's color was measured and identified in the CIE L*a*b* system. From Figure 6, it is shown that the film's color in this work was grey to gold-like as an increase of N_2 flow rates (Table 3). The close to 24K gold films was obtained by using the N_2 gas flow rates at 3.0 and 4.0 sccm with L* around 60, a* around 6, and b* around 26 - 28. The results are in good agreement with a study that the film's color changes totally from grey to golden as the change in the N/Ti ratio (Grosso et al., 2017). In addition, the golden color is obtained as the stoichiometric titanium nitride. Depending on the stoichiometry variations in the number of free-electron are obtained that play a role in the reflection of light (Bendavid, Martin, Netterfield, & Kinder, 1996).

Suan Sunandha Science and Technology Journal

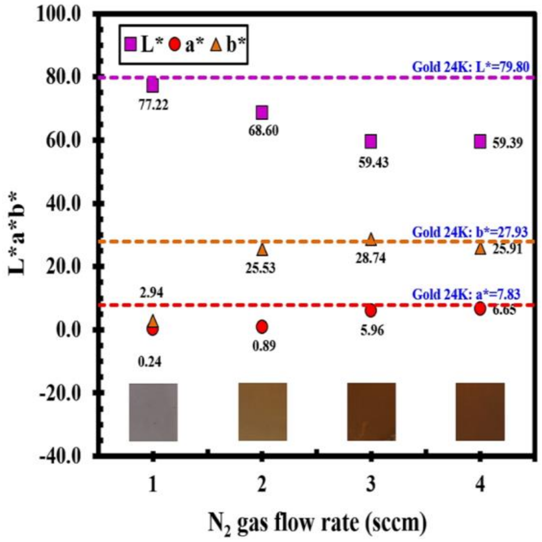

Figure 6. The Color of TiN films measured in the CIE L*a*b* system as a function of the N_2 flow rates.

4. Conclusion

The TiN thin films were successfully prepared by using DC reactive magnetron sputtering at different N_2 flow rates at 1.0-4.0 sccm in 1.0 sccm increments. The crystal structures, microstructures, surface morphologies, elemental compositions, and color were strongly influenced by the N_2 gas flow rates. The results showed the as-deposited thin films had a B1-NaCl structure of TiN(111), TiN(200), TiN(220), and TiN(311). The lattice constants were in the range of 4.211-4.239 Å. The crystal sizes were as small as below 25 nm. The thickness reduced from 1254 nm to 790 nm, with opposite change of the N_2 flow rate. The concentration of Ti and N in the films (Ti and N contents) depended on the N_2 flow rates. From the cross-sectional analysis, the films showed the changing of the structure from the dense to the compact columnar. The hardness obtained by the nano-indentation technique was increased from 4 - 19 GPa with following in the N_2 flow rates. The color close to 24K gold thin films was obtained by using the N_2 gas flow rates at 3.0 and 4.0 sccm.

References

Ajenifuja, E., Popoola, A. P. I., & Popoola, O. M. (2019). Thickness dependent chemical and microstructural properties of DC reactive magnetron sputtered titanium nitride thin films on low carbon steel cross-section. *Journal of Materials Research and Technology*, *8*(1), 377-384. doi:10.1016/j.jmrt.2018.02.010

Bendavid, A., Martin, P. J., Netterfield, R. P., & Kinder, T. J. (1996). Characterization of the optical properties and composition of TiN_x thin films by spectroscopic ellipsometry and X-ray photoelectron spectroscopy. *Surface and Interface Analysis*, *24*(9), 627-633. doi:10.1002/(SICI)1096-9918(19960916)24:9<627::AID-SIA149>3.0.CO;2-R

Gao, F., & Sun, W. (2019). Nonlinear finite element modeling and vibration analysis of the blisk deposited strain-dependent hard coating. *Mechanical Systems and Signal Processing*, *121*, 124-143. doi:10.1016/j.ymssp.2018.11.028

Grosso, S., Latu-Romain, L., Berthome, G., Renou, G., Le Coz, T., & Mantel, M. (2017). Titanium and titanium nitride thin films grown by dc reactive magnetron sputtering Physical Vapor Deposition in a continuous mode on stainless steel wires: Chemical, morphological and structural investigations. *Surface and Coatings Technology*, *324*, 318-327. doi:10.1016/j.surfcoat.2017.05.089

Jithin, M., Ganapathi, K. L., Vikram, G. N. V. R., Udayashankar, N. K., & Mohan, S. (2018). Pulsed DC magnetron sputtered titanium nitride thin films for localized heating applications in MEMS devices. *Sensors and Actuators A: Physical*, *272*, 199-205. doi:10.1016/j.sna.2017.12.066

Kim, S. H., Park, H., Lee, K. H., Jee, S. H., Kim, D. J., Yoon, Y. S., & Chae, H. B. (2009). Structure and mechanical properties of titanium nitride thin films grown by reactive pulsed laser deposition. *Journal of Ceramic Processing Research*, *10*(1), 49-53.

Kumar, D. D., Kumar, N., Kalaiselvam, S., Thangappan, R., & Jayavel, R. (2018). Film thickness effect and substrate dependent tribo-mechanical characteristics of titanium nitride films. *Surfaces and Interfaces*, *12*, 78-85. doi:10.1016/j.surfin.2018.05.002

Kusano, E. (2019). Structure-zone modeling of sputter-deposited thin films: A brief review. *Applied Science and Convergence Technology*, *28*(6), 179-185.

Lepicka, M., Gradzka-Dahlke, M., Pieniak, D., Pasierbiewicz, K., Krynska, K., & Niewczas, A. (2019). Tribological performance of titanium nitride coatings: A comparative studyon TiN-coated stainless steel and titanium alloy. *Wear*, *422-423*, 68-80.

Mitterer, C. (2014). PVD and CVD hard coatings. In V. K. Sarin (Ed.), *Comprehensive hard materials* (pp. 449-467). Oxford, UK: Elsevier. doi:10.1016/B978-0-08-096527-7.00035-0

Pelleg, J., Zevin, L. Z., Lungo, S., & Croitoru, N. (1991). Reactive-sputter-deposited TiN films on glass substrates. *Thin Solid Films*, *197*(1-2), 117-128. doi:10.1016/0040-6090(91)90225-M

Ponon, N. K., Appleby, D. J. R., Arac, E., King, P. J., Ganti, S., Kwa, K. S. K., & O'Neill, A. (2015). Effect of deposition conditions and post deposition anneal on reactively sputtered titanium nitride thin films. *Thin Solid Films*, *578*, 31-37. doi:10.1016/j.tsf.2015.02.009

Santecchia, E., Hamouda, A. M. S., Musharavati, F., Zalnezhad, E., Cabibbo, M., & Spigarelli, S. (2015). Wear resistance investigation of titanium nitride-based coatings. *Ceramics International*, *41*(9), 10349-10379. doi:10.1016/j.ceramint.2015.04.152

Thampi, V. V. A., Bendavid, A., & Subramanian, B. (2016). Nanostructured TiCrN thin films by Pulsed Magnetron Sputtering for cutting tool applications. *Ceramics International*, *42*(8), 9940-9948. doi:10.1016/j.ceramint.2016.03.095

Zhang, D. H., Yang, T. L., Ma, J., Wang, Q. P., Gao, R. W., & Ma, H. L. (2000). Preparation of transparent conducting ZnO:Al films on polymer substrates by r. f. magnetron sputtering. *Applied Surface Science*, *158*(1-2), 43-48. doi:10.1016/S0169-4332 99 00591-7

Zhang, H., Li, Z., Ma, C., He, W., Cao, X., & Li, Y. (2019). The anti-sand erosion performance of TiN films fabricated by filtered cathodic vacuum arc technique at different nitrogen flow rates. *Ceramics International*, *45*(8), 10819-10825. doi:10.1016/j.ceramint.2019.02.157

Zhang, S., Yan, F., Yang, Y., Yan, M., Zhang, Y., Guo, J., & Li, H. (2019). Effects of sputtering gas on microstructure and tribological properties of titanium nitride films. *Applied Surface Science*, *488*, 61-69. doi:10.1016/j.apsusc.2019.05.148

Zhou, T., Liu, D., Zhang, Y., Ouyang, T., & Suo, J. (2016). Microstructure and hydrogen impermeability of titanium nitride thin films deposited by direct current reactive magnetron sputtering. *Journal of Alloys and Compounds*, *688*, 44-50. doi:10.1016/j.jallcom.2016.06.278